Preparation and Characterization of Iron(III) Complex of an Amino-Functionalized Polyacrylamide-Grafted Lignocellulosics and its Application as Adsorbent for Chromium(VI) Removal from Aqueous Media

Thayyath S. Anirudhan, Sreenivasan Rijith, Padmajan S. Suchithra

Department of Chemistry, University of Kerala, Kariavattom, Trivandrum 695 581, India

Received 21 April 2008; accepted 10 August 2009
DOI 10.1002/app.31275
Published online 7 October 2009 in Wiley InterScience (www.interscience.wiley.com).

ABSTRACT: This study concerns with the development of a new adsorbent, iron(III) complex of an amino-functionalized polyacrylamide-grafted coconut coir pith (CP), a lignocellulosic residue, for Cr(VI) in water and industry effluents. The adsorbent (AM-Fe-PGCP) was characterized by FTIR, EDS, Mössbauer, surface area analyzer, TG/DTG, and potentiometric titration. The effects of contact time, initial sorbate concentration, pH, dose of adsorbent, and temperature on Cr(VI) adsorption were studied to optimize the conditions for maximum adsorption. The kinetics of sorption was investigated using pseudo-first-order and pseudo-second-order rate equations with the later giving a better fit to the experimental data. The mechanism of sorption was found to be film diffusion controlled. The Langmuir isotherm model yields a much better fit than the Freundlich and Dubinin–Radushkevich models with maximum adsorption capacity of 142.76 mg/g at 30°C. Simulated industry wastewater sample was treated with AM-Fe-PGCP to demonstrate its efficiency in removing Cr(VI) from wastewater. The alkali treatment (0.1*M* NaOH) and re-introduction of Fe^{3+} lead to a reactivation of the spent adsorbent and can be reused through many cycles of water treatment and regeneration without any loss in the adsorption capacity. © 2009 Wiley Periodicals, Inc. J Appl Polym Sci 115: 2069–2083, 2010

Key words: lignocellulosics; graft copolymerization; chromium(VI) adsorption; isotherm; desorption

INTRODUCTION

Chromium is a toxic heavy metal that is widely used in electroplating, leather tanning, metal finishing, nuclear power plant, textile industries, and chromate preparation.[1] It occurs in Cr(III) and Cr(VI) forms. Cr(III) is an essential element but is toxic at its higher concentration. Cr(VI) is a well-known highly toxic metal, considered as a priority pollutant. The maximum permissible levels of Cr(VI) in drinking and industrial wastewater were set by the Environmental Protection Agency (EPA) to be 0.05 and 0.20 mg/L, respectively.[2] The best way to reduce the contamination load of water is the effective removal of metal ions. Several agricultural by-products (lignocellulosics) have been investigated as adsorbents for removing metals from water and wastewater and has been reviewed by Babel and Kurniawan.[3] The application of these lignocellulosic materials has been found to be limited due to leaching of some organics, into the solution. Grafting polymer chains onto the backbone of lignocellulosic materials has been pointed out as a convenient method for improving physical, chemical, and mechanical properties of such materials and also to increase their adsorption capacities as well as to prevent the leaching of organics. A number of ion exchange resins with different functionalities have been developed from certain lignocellulosic materials (saw dust, bagasse pith, banana stalk, banana stem, and wood pulp) using graft copolymerization reaction for the removal of heavy metals from aqueous solutions.[4–8]

Graft copolymerization of acrylamide (AAm) onto cellulose, saw dust, and banana stalk was investigated by earlier works.[9–11] AAm was chosen as monomer because it readily graft copolymerizes onto cellulosic materials in the presence of a number of initiating systems including peroxides, persulfates, redox couples, azo compounds, and photochemicals.[12] Also the formation of the chemical and physical network structures in acrylamide polymers has advantages in many applications such as water treatment, chromatography, and super absorbent polymer technology. The free-radical crosslinking copolymerization of AAm with *N*,*N*′-methylenebisacrylamide is the usual way to build up AAm polymer networks. According to Flory's[13] network

Correspondence to: T. S. Anirudhan (tsani@rediffmail.com).

theory, crosslinking density is a key factor influencing adsorption capacity. Crosslinking reduces the solubility of biomass in aqueous solvents at low pH and can improve the mechanical properties, resistance to chemical and surface area.[14,15] Infact, due to large specific surface area and strong mechanical strength of crosslinked products, they can be applied to metal ion recovery.

Generally, the nitrogen atom from the amide group lacks sufficient electron donating character due to the adjacent electron withdrawing carbonyl group, and it cannot normally form coordination bonds with transition metal ions. According to the theory of hard and soft acid and bases (HSAB) defined by Pearson,[16] metal ions will have a preference for complexing with ligands that have more or less electronegative donor atoms (N and S). Divinylbenzene-crosslinked polyacrylamide beads modified with ethylenediamine (transamidation) to get amine group have been used to remove metal ions such as Co(II), Ni(II), Cu(II), Zn(II), and Hg(II).[17] The amine groups that can make coordination bond with cationic metal due to the presence of lone pair of electrons in sp^3 hybridized amine nitrogen. In a previous research, it was demonstrated that Cu(II)-coordinated amino-functionalized mesoporous silica is an excellent adsorbent for the removal of arsenate and chromate ions based on cation–anion interaction.[18] According to HSAB theory, iron(III) is classified as a hard acid, hard acids form very strong bonds with amine group (hard base).[19] In this study, iron(III)-loaded amine-modified polyacrylamide coconut coir pith (CP) was prepared and used in the removal of Cr(VI) from aqueous solutions. Since the coordination number of Fe^{3+} (d^5) complex is 6 and after its coordination with amine groups residual Fe^{3+} adsorption sites are expected to show high Cr(VI) binding ability.

CP is a widely available and abundant natural material, which basically contain cellulose and lignin. India, the third largest producer of coconut in the world, produces 7.5 million tones CP as a waste generated in the process of separation of fiber from coconut husk. Any attempt to reutilize this agro waste will be worth while. One of the ways of efficient and environment friendly utilization of biomass waste is its conversion into adsorbents. The results of the earlier study showed that the product obtained from modified CP exhibits outstanding adsorption capacity for arsenate(V) from aqueous solutions.[20]

In this work, we have prepared a novel adsorbent iron(III) complex of an amine-modified polyacrylamide-grafted CP (AM-PGCP) by means of a simple graft copolymerization reaction of acrylamide and CP using MBA as a crosslinker and potassium persulfate as an initiator followed by ethylenediamine treatment (transamidation) and iron(III) loading in the presence of HCl, and it is used for the effective removal of Cr(VI) from various aqueous media.

EXPERIMENTAL

Preparation of adsorbent

The CP used as a starting material for the preparation of adsorbent. It was procured from a local coir industry and washed several times with distilled water to remove surface adhered particles and soluble materials. CP was oven-dried, ground, and sieved using standard test sieves to approximate the particle diameter of 0.096 mm. Determination of composition of CP basically comprises α-cellulose, hemicellulose, and lignin using the standard method described by Ott[21] and were found to be 46.1, 18.7, and 27.3% respectively. Hydroxyl groups present in the cellulosic residues in CP enhances the graft polymerization. Scheme 1 represents the general procedure adopted for the preparation of adsorbent. Twenty grams of CP immersed in 200 mL distilled water in 1 L reaction flask, in which 2.5 g *N*,*N*′-methylenebisacrylamide (MBA) was added as a crosslinking agent and 1.0 g potassium peroxydisulfate ($K_2S_2O_8$) was added as initiator, stirred well for 5 min. Purified N_2 was passed through the vessel for 10 min. The polymerization was started by adding 25 g of acrylamide (AAM) monomer. The mixture was stirred regularly at 70°C in a water bath until a solid mass was obtained. The water soluble homopolymer was removed and the polyacrylamide-grafted CP (PGCP) obtained was collected. The quantity of grafted monomer (graft yield) was evaluated as the weight increase of the sample after the extraction of the homopolymer; it is expressed as the percentage increase of weight:

$$\text{Graft yield}\,(\%) = \frac{(w_1 - w_2) \times 100}{w_1} \qquad (1)$$

where w_1 is the initial weight of the sample and w_2 is the grafted weight of extracted sample. Grafting yield was determined and was found to be 78.8%. The dried mass was refluxed with 10 mL ethylenediamine (en) continuously for 8 h. The product, amine-modified PGCP (AM-PGCP) was separated and washed with toluene and then dried.

The batch adsorption isotherm experiments were used to investigate the operational conditions for maximum loading of iron(III) onto AM-Fe-PGCP. The adsorption isotherm of iron(III) by AM-PGCP was performed by agitating 0.1 g of AM-PGCP in 50 cm^3 of iron(III) solution of concentration varying between 10 and 300 mg dm^{-3} at 30°C and pH 3.0. Iron(III)

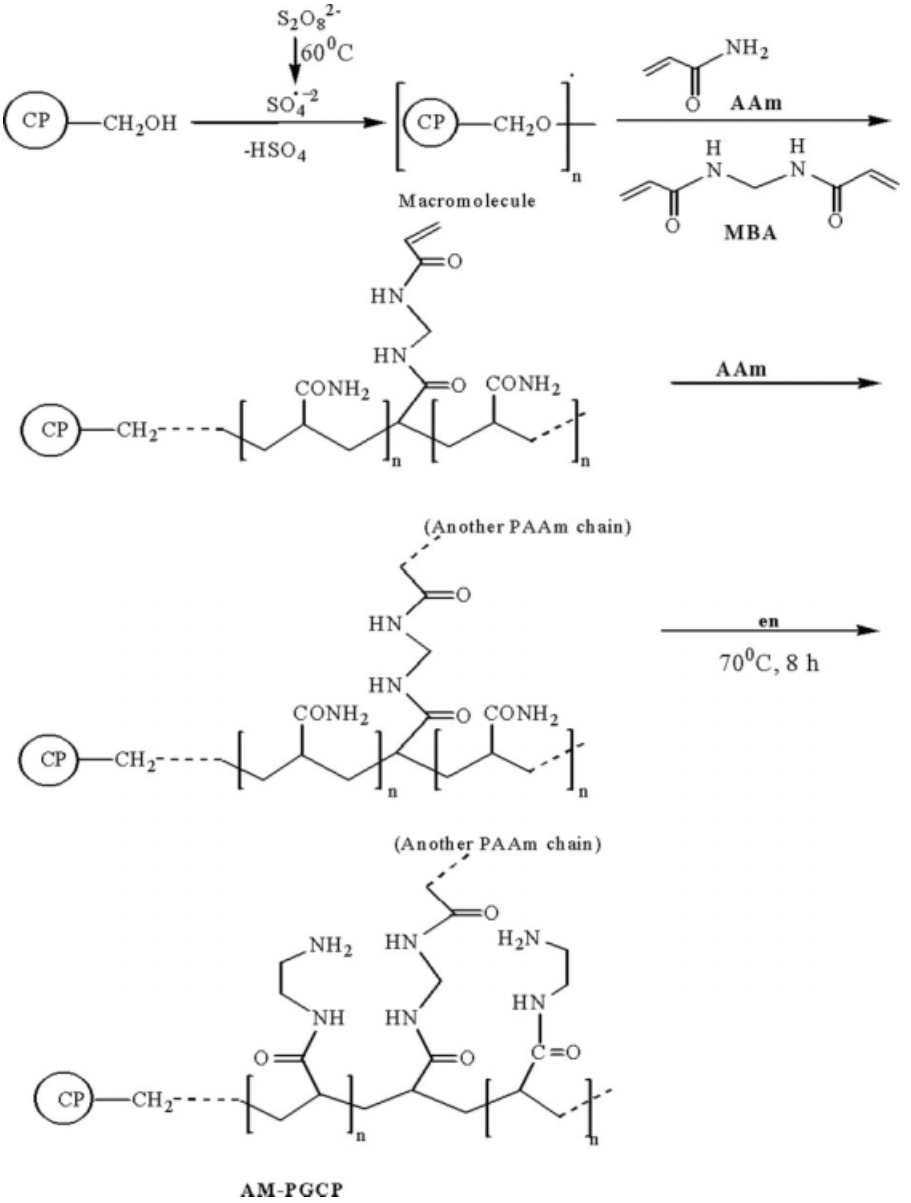

Scheme 1 Proposed mechanistic pathway for synthesis of AM-PGCP.

concentrations before and after adsorption were measured using a GBC Avanta–A 5450 atomic absorption spectrophotometer (AAS). Sorption capacity (q_e) of Fe(III) onto AM-PGCP was calculated by the mass balance equation, $q = (C_0 - C_e)V/w$, where V, w, C_0, and C_e, are the volume of solution (mL), the sorbent mass (g), and the initial and equilibrium concentrations (mg/L), respectively. The product, Fe(III)-loaded AM-PGCP (AM-Fe-PGCP) was filtered, washed with water, and dried at 60°C for 24 h. The adsorbent with an average particle size of 0.096 mm was used for further adsorption experiments.

Equipments and method of characterization

The IR spectra of the CP and AM-Fe-PGCP were recorded on a Schimadzu FTIR spectrophotometer model 1801 using pressed disk technique. Element distributions were estimated on each section by an X-ray Energy Disperse Scattering analysis (EDS) using a JSM 6390 LV SEM at 20 keV with background subtraction and a summation of 60 scans. The surface area of the CP, AM-PGCP, and AM-Fe-PGCP was obtained from adsorption and desorption of N_2 at 77 K using Quantasorb surface area analyzer (Model QS-7). Mössbauer spectra were obtained at room temperature using a constant acceleration transmission spectrometer equipped with a ^{57}Co/Rh source of about 20 mCi.

The point of zero charge (pH_{pzc}) is defined as the pH of the suspension at which surface charge density $\sigma_0 = 0$. A potentiometric titration method[22] was employed to determine the values of pH_{pzc}. The amine content of the AM-PGCP was estimated in

accordance with the acid titration procedure described by Zu and Alexandratos.[23] The apparent density of the adsorbents was determined using specific gravity bottles. A systronic microprocessor pH meter (model, 362, India) was used to measure the potential and pH of the suspension. For kinetic and isotherm studies, a Labline temperature controlled water bath shaker with a temperature tolerance of ±1.0°C was used. The concentration of iron(III) in solution was determined using a GBC Avanta-A5450 atomic absorption spectrophotometer (AAS). Residual chromium(VI) concentrations after adsorption were analyzed spectrophotometrically[24] by monitoring the absorbance using UV–visible spectrophotometer (Jasco model V 530).

Adsorption experiments

The Cr(VI) stock solution (1000 mg/L) was prepared in distilled water with analytical-grade potassium dichromate ($K_2Cr_2O_7$, from Aldrich Company). Batch adsorption experiments were conducted in 100 mL flasks each of which containing 50 mL of Cr(VI). Hundred milligrams of adsorbent were added into each flask and contents in the flasks were shaken in a thermostatic shaker at 30°C and 200 rpm. The pH of the solutions was adjusted by using 0.1*M* HCl or 0.1*M* NaOH. Liquid samples were withdrawn at predetermined time intervals and centrifuged for 10 min at 1000 rpm. The concentration of the Cr(VI) remaining in the supernatant was determined spectrophotometrically using 1,2-diphenyl carbazide as a chromogenic reagent. The amount of Cr(VI) adsorbed onto AM-Fe-PGCP was calculated from the difference between the initial concentration and the final concentration. Total chromium (Cr(III) and Cr(VI)) was determined using AAS. The difference in concentration between total and Cr(VI) was taken as the concentration of Cr(III). The investigation for the effect of solution pH values on chromium adsorption was conducted at initial chromium concentrations of 50 and 100 mg/L, but the pH value ranged from 2.0 to 9.0. For the adsorption isotherm experiments, the initial solution pH was 4.0, while the initial chromate concentration in the solution varied between 100 and 600 mg/L. In all experiments, one control was maintained without adsorbent.

Desorption and regeneration studies

Desorption studies were conducted by batch experiments. After performing adsorption experiments with 100 mg/L of Cr(VI) solution, the Cr(VI) loaded adsorbent was separated. The spent adsorbent was gently washed with distilled water to remove unadsorbed Cr(VI) ions. The exhausted adsorbent was added to desorption medium and shaken for 2 h. The amount of Cr(VI) ions onto the solution was determined using the procedure as described earlier. The adsorbent was subjected to the subsequent Cr(VI) loading cycle. The reusability of the adsorbent was further confirmed by repeating the adsorption–desorption cycle up to four times, thereby checkout the long-term adsorption performance of AM-Fe-PGCP.

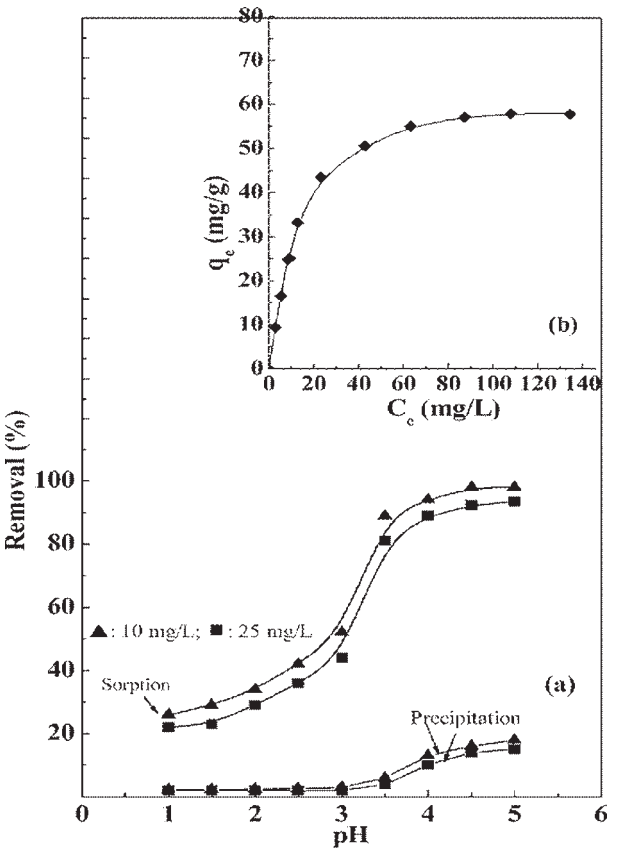

Figure 1 (a) Effect of pH and (b) isotherm profile for Fe(III) adsorption onto AM-PGCP ((a) adsorbent dose 2 g/L, equilibrium time 2 h; (b) adsorbent dose 2 g/L, equilibrium time 2 h, pH 3.0).

RESULTS AND DISCUSSION

Iron(III) adsorption profile onto AM-PGCP

To optimize the pH value for Fe(III) loading onto AM-PGCP from aqueous solution experimental data were carried out by varying the pH over the range 1.0–5.0 [Fig. 1(a)]. For comparison, iron hydroxide precipitation by NaOH is also given in Figure 1(a). It was observed that the percentage adsorption of Fe(III) increases with increasing pH and reached maximum at pH 5.0. It can also be shown that at any pH, in the range 3.5–5.0, Fe(III) removal by adsorption onto AM-PGCP is very much greater

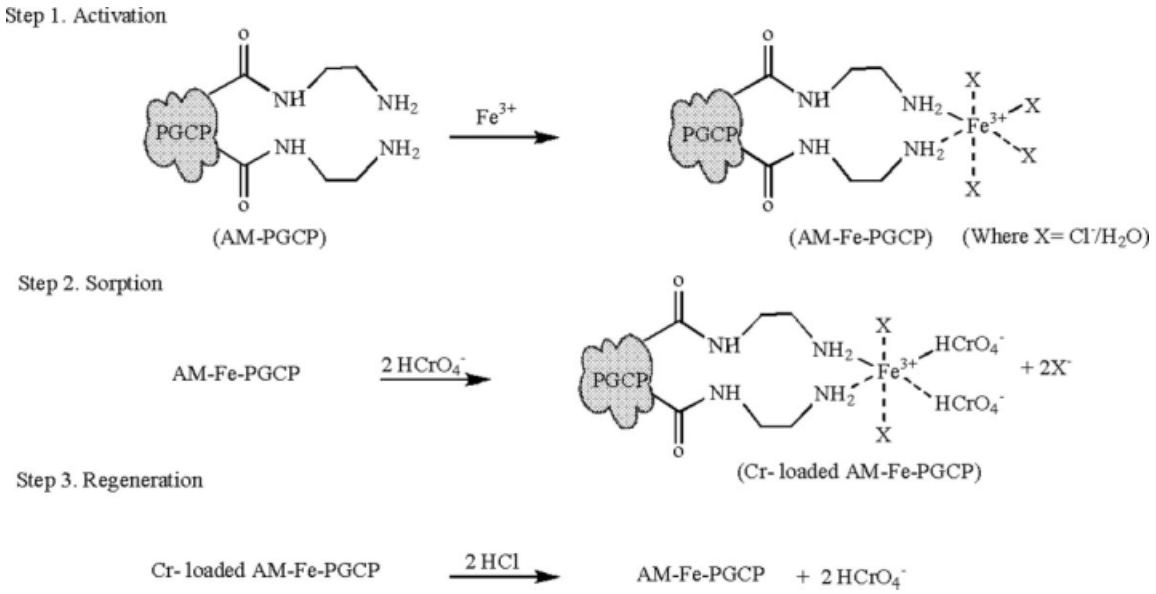

Scheme 2 Activation and regeneration cycles of AM-Fe-PGCP.

than the removal by hydroxide precipitation observed in the absence of adsorbent. As a result of hydrolysis of Fe(III), formation of stable iron complexes such as $Fe(OH)_3$ and $FeOH_4^-$ suppresses the iron adsorption at pH > 3.0. The low adsorption at low pH values (<3.0) can be attributed to the nature of the adsorbent and Fe(III) ions. In highly acidic solution, a strong competition exhibited between Fe(III) cations and protons for adsorption sites and the uptake capacity was decreased. Moreover, the amine groups of AM-PGCP are fully protonated at low pH values and thus the adsorbent is not active for the uptake of Fe(III) cations. As the pH gradually increases, amine groups are deprotonated and become available for chelation with Fe(III) ions, leading to an increase in adsorption.

Isotherm experiments were conducted to determine the Fe(III) loading capacity of the prepared AM-PGCP to check the adsorption capacity. The isotherm plot at 30°C [Fig. 1(b)] shows that the curvature of the isotherm is positive, regular, and concave to the concentration axis, which seems to be an L-type profile according to the classification of Giles et al.[25] Maximum monolayer coverage of Fe(III) was calculated and found to be 57.80 mg/g. From these results, AM-Fe-PGCP was prepared with maximum amount of Fe(III) at optimum concentration and pH to further investigate its adsorption capacity toward Cr(VI) ions.

Adsorbent characterization

The AM-Fe-PGCP contains both amide and amine functional groups. The amide nitrogen atom lacks sufficient electron donating character due to the adjacent electron withdrawing carbonyl group, and it cannot normally protonated in acidic medium. Since amide groups are not interacted with HCl,

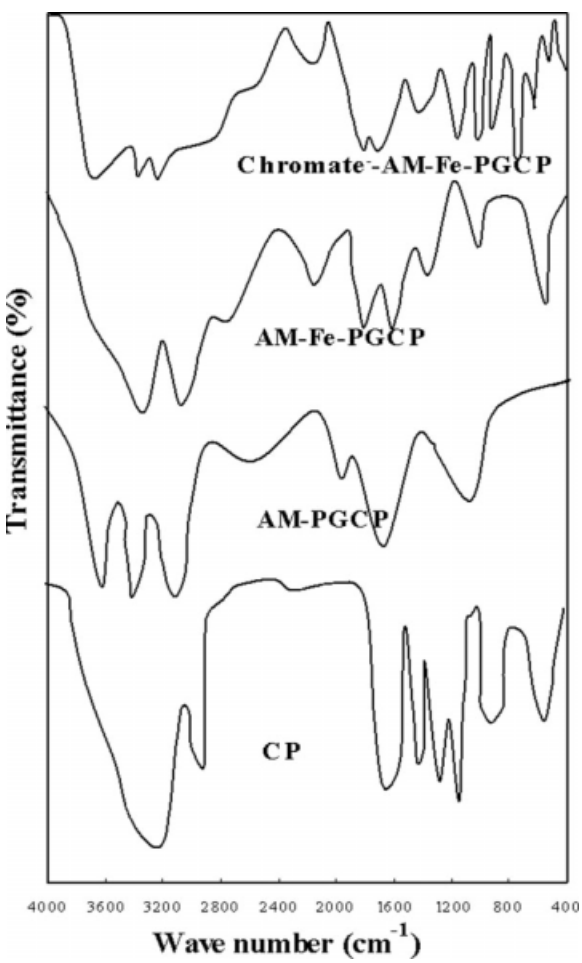

Figure 2 FTIR spectra of CP, AM-PGCP, AM-Fe-PGCP, and chromate-adsorbed AM-Fe-PGCP.

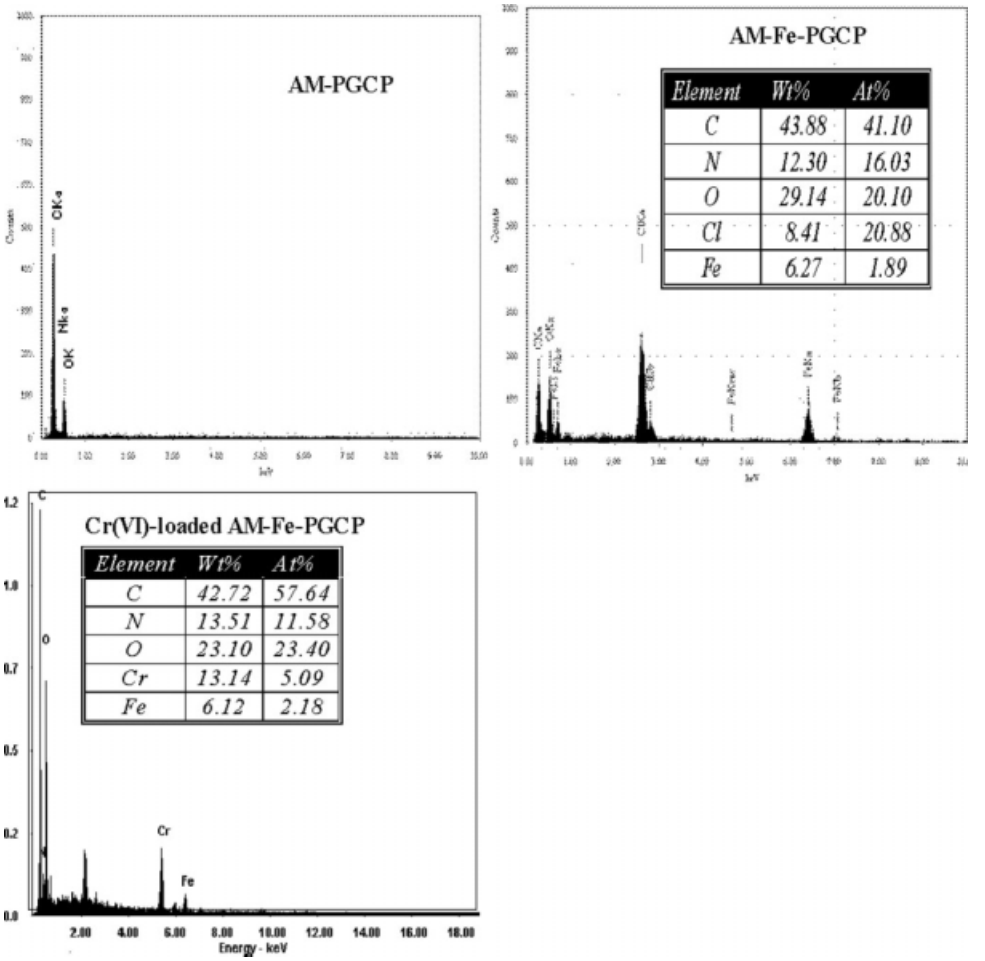

Figure 3 EDS surface analysis of AM-PGCP, AM-Fe-PGCP, and Cr-loaded AM-Fe-PGCP.

acid titration procedure[23] was used to determine amine groups in the presence of amide groups on the surface of the adsorbent. Earlier workers[17] also used same acid titration procedure for the estimation of amine groups in the presence of amide groups on the surface of the adsorbents. The density of amine groups in AM-Fe-PGCP was determined using the acid titration procedure and was found to be 2.38 mequiv/g. The maximum iron(III) loading in AM-Fe-PGCP calculated from isotherm curve was found to be 1.04 mequiv/g. From these results, molar ratio of amine to iron(III) in AM-Fe-PGCP was approximately 2 : 1 indicating that two ethylenediamine groups are involved to bind one Fe(III) ion (Scheme 2). The coordination number of Fe in iron (III) (d^5) complexes is 6 and to complete the coordination sphere; it is believed that Cl^- and/or H_2O molecules are coordinated to iron(III), which may act as ligands to replace Cr(VI) ions from aqueous solutions (Scheme 2).

The FTIR spectra of pure CP, AM-PGCP, AM-Fe-PGCP, and chromate-adsorbed AM-Fe-PGCP are presented in Figure 2. The spectrum of AM-PGCP exhibits many alterations from that of CP. The major differences are: The wide adsorption peak at 3280 cm^{-1}, corresponding to the hydrogen bonded stretching vibration from cellulose structure of the CP, splits into doublets at 3315 and 3740 cm^{-1}. The absorption band at 2920 cm^{-1}, assigned to C—H stretching vibration in CP, shows a significant shift to higher wave number 2980 cm^{-1}. New absorption bands observed in the spectrum of AM-PGCP at 3315 and 1665 cm^{-1}, which are assigned to stretching vibrations of N—H and C=O of amide group. The additional bands appeared at 1620 and 1060 cm^{-1} are assigned to N—H bending and C—N stretching vibrations, respectively, corresponding to an amine group bonded to the PGCP through transaimidation reaction. These results indicate that grafting might have occurred at the O—H sites of the cellulose and also the presence of amine functionality in the AM-PGCP.

After Fe(III) loading, the absorption bands of N—H at 1620 and 3315 cm^{-1} shifted to lower wave numbers 1598 and 3291 cm^{-1} and a new band of Fe—N stretching appeared at 448 cm^{-1}. This information reveals that amine groups took part in Fe(III) coordination. Generally, the amide nitrogen atom

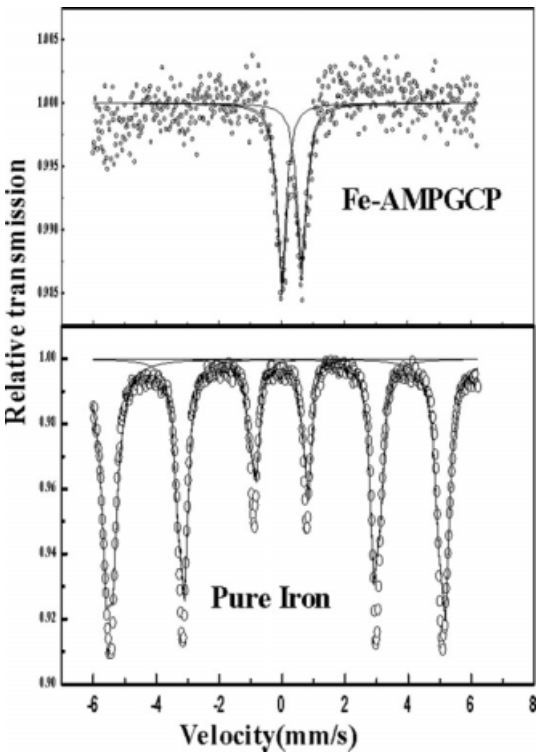

Figure 4 Mössbauer spectrums of pure iron and Fe-loaded AM-PGCP.

lacks sufficient electron donating character due to the adjacent electron withdrawing carbonyl group, and it cannot normally form coordination bonds with Fe(III). In the spectrum recorded after Cr(VI) adsorption onto AM-Fe-PGCP, new bands that belong to the Cr—O and Cr=O stretching, respectively, appear at 783 and 906 cm^{-1}.

The EDS spectrum of AM-PGCP, AM-Fe-PGCP, and Cr(VI)-loaded AM-Fe-PGCP is shown in Figure 3. The principle constituents such as C, N, and O are present in AM-PGCP, AM-Fe-PGCP, and Cr(VI)-loaded AM-Fe-PGCP. The EDAX analysis (Fe and Cl peaks) of AM-Fe-PGCP clearly shows the appearance of Fe(III) and exchangeable chloride ligands as a result of iron loading. Chloride peaks were present due to the addition of hydrochloric acid during iron(III) loading. After Cr(VI) adsorption, the chloride peaks present in AM-Fe-PGCP were disappeared and new peaks of Cr(VI) were found in Cr(VI)-loaded AM-Fe-PGCP and this clearly indicates that the ligand exchange mechanism contributes to the adsorption process. This reinforces the possibility of an anion exchange mechanism explained in Schemes 1 and 2 for the accumulation of chromium onto AM-Fe-PGCP. According to these EDAX spectra, the molar ratio of [Fe] : [Cl] in AM-Fe-PGCP was 1.2 : 2.4 and the molar ratio of [Fe] : [Cr(VI)] in Cr(VI)-loaded AM-Fe-PGCP was 1.3 : 2.5, which indicates the evenly distribution of chloride and Cr(VI) on the surface of AM-Fe-PGCP.

Mössbauer spectra of the pure iron and AM-Fe-PGCP taken at room temperature are shown in Figure 4. Symmetric doublet is observed in the spectrum of AM-Fe-PGCP. It has an isomer shift of about 0.36 mm/s that is characteristic for high-spin Fe^{3+} in octahedral coordination.[26,27] Mössbauer spectrum of AM-Fe-PGCP shows that the quadrupole splitting of Fe^{3+} increases with increasing distortion of the coordination octahedron around Fe^{3+} environment.[28,29] The measured quadrupole splitting value is in the lower range (0.60–0.64 mm/s), which was typical for octahedrally coordinated Fe^{3+}. Spectral area ratios of the magnetically ordered component with lower quadrupole shift are indicative of a more symmetric environment. Although many published Mössbauer spectra show the same spectral symmetry, no explanation has so far been offered for this phenomenon, and published spectra have always been fit with only one sextet, indicating a single Fe site. Spectrum at 300 K exhibits two doublets which are well reproduced using two nonequiprobable quadrupolar components Γ1 (0.36 mm/s) and Γ2 (0.38 mm/s) indicating the symmetric environment of coordinated iron in AM-Fe-PGCP.

The TG/DTG analysis is a simple and accurate method for studying the decomposition pattern, effect of modification, and thermal stability of the adsorbents. Figure 5 shows the TG and DTG curves of CP, AM-PGCP, and AM-Fe- PGCP. The weight loss of the CP was around 70.3% in the heating process of up to 800°C. In the initial stage of decomposition (T_1 = 80°C), a weight loss of 5.9% is observed due to the decomposition of adsorbed water. In the second stage (T_2 = 332°C), 49.3% is lost due to the splitting of the cellulose structure and the chain

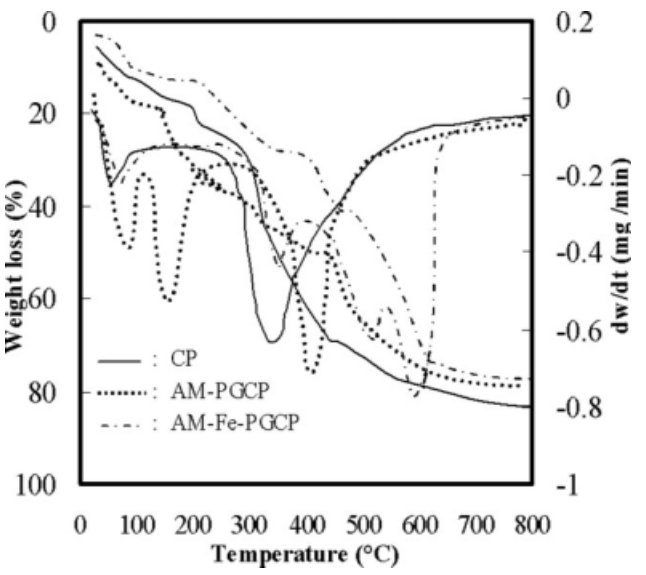

Figure 5 TG and DTG curves of CP, AM-PGCP, and AM-Fe-PGCP.

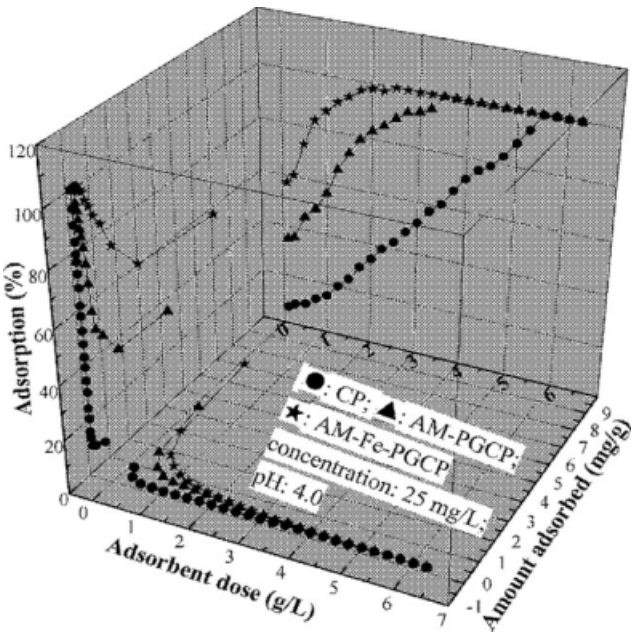

Figure 6 Effect of adsorbent dose on the adsorption of Cr(VI) onto CP, AM-PGCP, and AM-Fe-PGCP.

scission and breaking of some carboxyl and carbonyl bonds in the ring structure evolving CO, CO_2, and water and condensed tar by-products leaving behind rigid carbon skeleton. In the case of AM-PGCP, the initial decomposition temperature (T_1) is 85°C, where a weight loss 4.4% is observed due to the loss of adsorbed water. Second stage reaction between 180 and 410°C (T_2 = 346°C) where 40.2% of the dry weight loss was observed due to the release of water and CO_2 by the pyrolytic decomposition of cellulose unit and reorganization of carbon skeleton. In the third stage between 410 and 680°C (T_3 = 449°C) where 63.0% weight loss is observed due to the pyrolytic decomposition process in lignin and destruction of aminated fraction. The TG and DTG curves of AM-Fe-PGCP showed weight loss at four different temperature ranges with maximum decomposition temperatures 95°C (T_1), 386°C (T_2), 550°C (T_3), and 620°C (T_4). The first degradation was assigned to the dehydration (3.6%), the second degradation was attributed to the cellulose fraction (38.8%), and the third degradation was assigned to the aminated fraction of fibers (58.8%). The fourth degradation (60.8%) reveals the increased stability of AM-Fe- PGCP due to amination followed by Fe(III) loading. The thermal stability of the AM-Fe-PGCP is much better than that of AM-PGCP. This indicates that a stable structure is formed *in situ* during the course of Fe(III) loading and introduces thermal stability in the structure.

The values of pH_{pzc} were found to be 6.0, 7.4, and 7.7 for CP, AM-PGCP, and AM-Fe-PGCP, respectively. The AM-Fe-PGCP exhibits an amphoteric behavior, and it acts as a buffer in a wide pH range of 3–9 were the pH final remains almost close to pH_{pzc} for all values of $pH_{initial}$. Polymer grafting and Fe(III) loading reinforce the adsorbent surface with positive potential, and this facilitates the electrostatic interaction with anions. The values of surface area were 84.2, 36.5, and 29.8 m^2/g for CP, AM-PGCP, and AM-Fe-PGCP, respectively; the corresponding values of pore volume were 0.42, 0.33, and 0.29 cm^3/g. A variation in anion exchange capacity (0.32 mequiv/g for CP, 0.43 mequiv/g for AM-PGCP, and 0.73 mequiv/g for AM-Fe-PGCP) was also observed.

Effect of surface modification

The effect of surface modification on Cr(VI) adsorption was studied by conducting batch experiments using an initial concentration of 25 mg/L, with varying adsorbent doses of CP, AM-PGCP, and AM-Fe-PGCP (Fig. 6). It is apparent that by increasing the adsorbent doses of CP, AM-PGCP, and AM-Fe-PGCP the percentage of adsorption increases. When the dose increases, the active sites in the adsorbent increases, which facilitates the adsorption. However, if the adsorption capacity was expressed in milligram adsorbed per gram of adsorbent, the capacity decreased with increasing amount of adsorbent. This is mainly because of unsaturation of adsorption sites through the adsorption process.[30] Another reason may be due to the overlapping or aggregation of adsorption sites resulting in decrease in total surface area of the adsorbent available to Cr(VI) and an increase in diffusion path length. Among various adsorbents, AM-Fe-PGCP showed the highest uptake capacity. For the complete removal of Cr(VI) ions from an aqueous solution of 25 mg/L, a minimum adsorbent dosage of 2.5 g/L AM-Fe-PGCP, 3.5 g/L AM-PGCP, and 5.5 g/L CP was required. The results clearly indicate that AM-Fe-PGCP is 1.44 and 2.2 times more effective than AM-PGCP and CP,

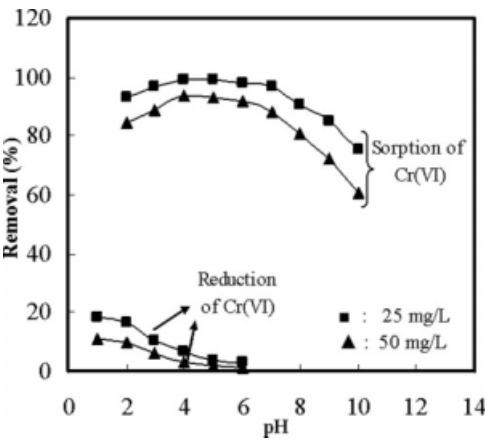

Figure 7 Effect of pH on the adsorption of Cr(VI) onto AM-Fe-PGCP (adsorbent dose 2.0 g/L, equilibrium time 2 h, and temperature 30°C).

respectively, for the removal of Cr(VI) ions. This may be due to the superior ligand exchange capacity and chelating capacity of AM-Fe-PGCP compared with CP and AM-PGCP because of the increasing number of ligands on AM-Fe-PGCP after grafting of acrylamide and iron(III) loading. Moreover, the modification caused a shift of pH_{pzc} from 6.0 in CP and 7.4 in AM-PGCP to 7.7 in AM-Fe-PGCP. The increase in pH_{pzc} also indicates that the surface becomes more positive due to iron(III) loading and the negatively charged Cr(VI) ions bind on these active surface sites through electrostatic interactions.

Effect of pH on Cr(VI) removal

The effect of pH on Cr(VI) removal by onto AM-Fe-PGCP was studied by varying the pH (2.0–10.0) of 25 and 50 mg/L initial concentrations and the results are presented in Figure 7. The results demonstrated that the adsorption percentage increases with pH and attained maximum at pH 4.0, later it was gradually declined. Depending on pH and Cr concentration,[31,32] the Cr(VI) species exist with equilibrium constant (at 25°C) as follows:

$$H_2CrO_4 \leftrightarrow H^+ + HCrO_4^- \qquad pK_1 = 6.51 \qquad (2)$$

$$2HCrO_4^{2-} \leftrightarrow Cr_2O_7^{2-} + H_2O \qquad pK_2 = 5.65 \qquad (3)$$

$$HCrO_4^- \leftrightarrow H^+ + CrO_4^{2-} \qquad pK_3 = 14.56 \qquad (4)$$

At pH 4.0, the dominant $HCrO_4^-$ species will adsorb on the positively charged surface of the AM-Fe-PGCP through the electrostatic interactions.[33] Low adsorption at higher pH values implies that CrO_4^{2-} ions compete with OH^- ions to the reaction sites of the adsorbent.[34] At lower pH values, $Cr_3O_{10}^{2-}$ and $Cr_4O_{13}^{2-}$ species are formed and these species are difficult to exchange with Cl^- ions from the adsorbent surfaces.

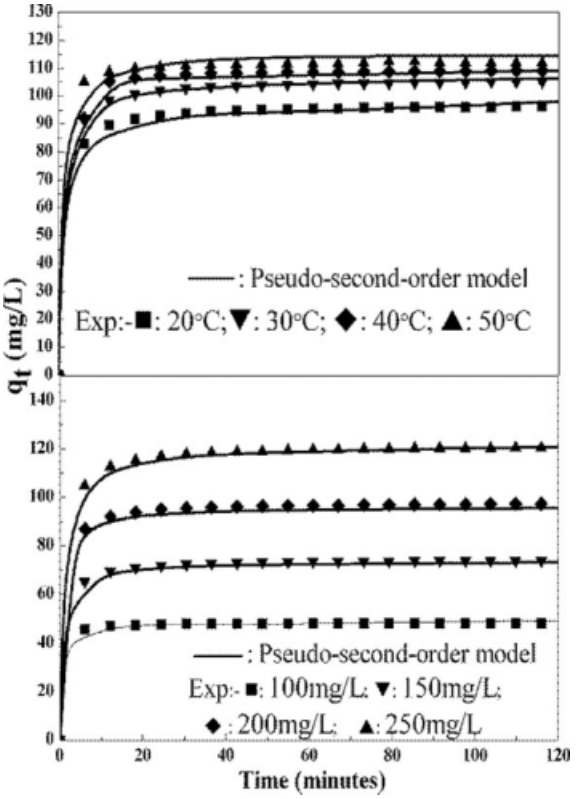

Figure 8 Effect of initial concentration, temperature with contact time of adsorption of Cr(VI) onto AM-Fe-PGCP, and comparison of observed data with pseudo-second-order kinetic model (adsorbent dose 2.0 g/L, pH 4.0).

The adsorption can be considered to be ligand exchange reaction between coordinated Cl^- ion and $HCrO_4^-$ species (Scheme 2). The reaction can be schematically represented as:

(5)

When the pH was below pH_{pzc}, the surface of the adsorbent becomes positively charged. At pH < 4.0, the removal of Cr(VI) by AM-Fe-PGCP was found to be affected by its reduction to Cr(III). Figure 7 demonstrates that the conversion of Cr(VI) to Cr(III) mainly depends on the pH of the solution. The lower the pH, the higher the efficiency of the Cr(VI) conversion. This can be explained by the basic character of nitrogen sites, which according to the Lewis base concept would provide a higher concentration of delocalized electrons that would promote a reductive environment.[35] Since the adsorbent surface exhibits positive charge, adsorption of Cr(III) cations is thermodynamically unfavorable, probably by electrostatic repulsion. To test this Cr content from the Cr-loaded AM-Fe-PGCP after Cr(VI) adsorption at different pHs was eluted with an alkaline sulfate eluent. After this separation, the concentrations of Cr(VI) and total Cr were determined. From these experiments, it was found that the concentration of Cr(VI) always equated that of total Cr, indicating that Cr(III) adsorption is not taken place at very low pHs. In view of electrostatic interaction between the sorbent-sorbate systems, it was decided to maintain the pH at 4.0 in further experiments.

Effect of contact time and initial concentration

Figure 8 shows the effect of contact time on the adsorption of Cr(VI). The amount of Cr(VI) adsorbed

TABLE I
Kinetic Parameters for the Adsorption of Cr(VI) Onto AM-Fe-PGCP at Different Temperatures and Concentrations

	Pseudo-first-order					Pseudo-second-order					
										Diffusion coefficients	
Variable	q_e exp (mg/g)	$k_1 \times 10^{-2}$ (min^{-1})	q_e cal (mg/g)	r^2	χ^2	$k_2 \times 10^{-2}$ (g/mg/min)	q_e cal (mg/g)	r^2	χ^2	$D_f \times 10^{-7}$	$D_p \times 10^{-9}$
Temperature (°C)											
20	98.01	1.75	10.28	0.90	3.7	0.98	97.14	0.99	0.05	2.71	1.72
30	104.28	1.77	16.36	0.95	5.2	1.02	105.10	0.99	0.31	3.35	1.97
40	111.87	2.14	17.17	0.96	6.4	1.84	109.53	0.99	0.61	4.01	2.30
50	115.27	2.51	28.71	0.92	4.5	2.10	115.29	0.99	1.23	4.51	2.51
Concentration (mg/L)											
100	49.75	0.9	9.80	0.87	5.6	5.6	49.09	0.98	0.92	3.65	4.60
150	74.63	1.1	13.5	0.89	7.6	2.6	72.71	0.99	0.79	4.10	3.45
200	98.04	1.2	18.4	0.92	9.5	1.3	96.97	0.99	0.25	4.28	2.76
250	121.95	1.4	33.5	0.91	4.6	0.7	118.44	0.99	1.01	4.45	2.30

very rapidly up to 30 min and slowly reaches saturation at about 2 h. Depending on the initial concentrations about 70–80% removal of Cr(VI) was achieved during the first 30 min of the contact time, whereas only 15–20% of additional removal occurred in within 2 h of contact time. We did not find any significant influence of contact time on the adsorption efficiency after contact time of 2 h. The initial concentration did not have a significant effect on the time to reach equilibrium. The time profile of Cr(VI) uptake is a single, smooth, and continuous curve leading to saturation, suggesting the cooperativity Cr(VI) on the surface of the adsorbent. The equilibrium time of 2 h can be considered very short, which is an economically favorable condition for the adsorbent described here. The removal efficiency of Cr(VI) after equilibrium was 49.09 mg/g (99.6%), 72.71 mg/g (98.08%), 96.97 mg/g (96.9%), and 118.44 mg/g (97.2%), respectively, at initial concentrations of 100, 150, 200, and 250 mg/L. The results show that an increase in the initial Cr(VI) concentration leads to an increase in the Cr(VI) uptake. The important driving force to overcome all mass transfer resistance between solid–liquid phase was the initial concentration of adsorbed species. Hence, a higher initial Cr(VI) concentration would enhance sorption process.

Adsorption kinetics

To evaluate kinetic mechanism that controls the adsorption process, Lagergren's pseudo-first-order, pseudo-second-order,[36,37] and diffusion kinetic models are tested to interpret the experimental data. The pseudo-first-order kinetic model equation is represented by

$$q_t = q_e[1 - e^{(-k_1 t)}] \tag{6}$$

where q_t and q_e are the amount of adsorbate sorbed at time t and at equilibrium respectively and k_1 is the pseudo-first-order rate constant (min^{-1}).

The pseudo-second-order kinetic model equation is expressed as

$$q_t = \frac{k_2 q_e^2 t}{1 + k_2 q_e t} \tag{7}$$

where q_e is the maximum adsorption capacity (mg/g) and k_2 is the equilibrium rate constant for pseudo-second-order adsorption (g/mg/min). Modeling of kinetic data was performed by a nonlinear regression method that involves the Levenberg–Marquardt method.[38] Correlation of kinetic data are presented in Table I. The theoretical q_e values as calculated from pseudo-second-order kinetic model agree perfectly with the experimental q_e values. This suggests that the sorption system is not a first-order reaction and that a pseudo-second-order model can be considered. The experimental q_t values are in good agreement with the calculated ones using pseudo-second-order kinetic equation (Fig. 8). The pseudo-second-order model is based on the assumption that the rate-limiting step may be a chemical sorption involving valance forces through sharing or exchange of electrons between adsorbent and adsorbate. It provides the best correlation of the data.

The adsorption mechanism could be controlled by reaction kinetics or by diffusion such as film or pore diffusion. To assess the nature of the diffusion process responsible for the adsorption of Cr(VI) ion on AM-Fe-PGCP, attempts were made to calculate the values of film diffusion coefficient (D_f) and pore-diffusion coefficient (D_p) at different temperatures and concentrations using the following equations:

$$D_f = 0.23 \frac{r_0 \delta \bar{C}}{t_{1/2} C} \tag{8}$$

$$D_p = 0.03 \frac{r_0^2}{t_{1/2}} \tag{9}$$

where r_0 is the radius of the adsorbent, $\bar{C}/C$ is the equilibrium loading of the adsorbent, and δ is the film thickness. Assuming spherical geometry for the sorbent, thickness of the film is taken as 10^{-3} cm, as reported by earlier workers.[39,40] According to them film diffusion to be rate-limiting, the values of D_f should be in the range 10^{-6} to 10^{-8} cm^2/s. For pore diffusion to be rate-limiting, the values of D_p should be in the range 10^{-11} to 10^{-13} cm^2/s. The kinetic data obtained for different initial concentrations and temperatures were used to calculate diffusion coefficients for the adsorption of Cr(VI) onto AM-Fe-PGCP (Table I). When the concentration of Cr(VI) increases from 100 to 250 mg/L, the value of D_f increases from 3.65×10^{-7} to 4.45×10^{-7} cm^2/s; whereas the value of D_p decreases from 4.60×10^{-9} to 2.30×10^{-9} cm^2/s. The value of D_f increases from 2.71×10^{-7} to 4.51×10^{-7} cm^2/s when the temperature increases from 20 to 50°C; but the corresponding D_p value increases from 1.72×10^{-9} to 2.51×10^{-9} cm^2/s. The increased mobility of ions and a decrease in retarding forces acting on the diffusing ions result in the increase of diffusion coefficients with temperature. It is evident that the rate-limiting step appears to be the film diffusion process, since the magnitude of the coefficients is in the range 10^{-6} to 10^{-8} cm^2/s.

The influence of the initial concentration of Cr(VI) on rate constant reveals the decreasing tendency of rate, which can be interpreted by the existence of Cr(VI) species in solution. According to the equilibrium relationship,[41] at lower initial concentration, $HCrO_4^-$ is the predominant species which can easily move toward the AM-Fe-PGCP surface. As the initial concentration increases the concentration of $HCrO_4^-$ is an increase, but a less amount of $Cr_2O_7^{2-}$ ions also coexisting with $HCrO_4^-$ ions. Large-sized $Cr_2O_7^{2-}$ ions (7.3×10^{-3} m^3/mol) move slowly when compared with the small-sized $HCrO_4^-$ (4.4×10^{-3} m^3/mol).[42] Again, the interelectronic repulsive force increases with an increase in $Cr_2O_7^{2-}$ ion concentration, which retard the transport rate of $HCrO_4^-$ ion. Therefore, the value of rate constant decreases with increase in concentration.

Adsorption isotherm study

To optimize the design of an adsorption system for the adsorption of adsorbates, it is important to establish the most appropriate correlation for the equilibrium curves. Adsorption isotherms of Cr(VI) onto AM-Fe-PGCP at differential temperatures are shown in Figure 9. Isotherm equations such as Langmuir, Freundlich, and Dubinin–Radushkevich have been used to describe the equilibrium characteristics of adsorption. The mathematical expression of the Langmuir model is

$$q_e = \frac{Q_0 b C_e}{1 + b C_e} \tag{10}$$

where q_e and C_e are the amount adsorbed (mg/g) and sorbate concentration in solution (mg/L), both at equilibrium. Q_o is the monolayer capacity of the adsorbent (mg/g) and b is the energy of adsorption (L/mg). A basic assumption in the Langmuir theory is that sorption takes place at specific homogeneous sites within the adsorbent. The empirical Freundlich expression is an exponential equation, and therefore assumes that as the adsorbate concentration increases so too does the concentration of adsorbate on the adsorbent surface. The Freundlich adsorption isotherm can be expressed as:

$$q_e = K_F C_e^{1/n} \tag{11}$$

where K_F is the Freundlich adsorption constant, which is a comparative measure of the adsorption capacity of the adsorbent and $1/n$ is an empirical constant indicates the intensity of the adsorption. The magnitude of the n gives an indication of the favorability of the adsorbent/adsorbate system. Values of $n > 1$ are usually termed as favorable adsorption.

D–R isotherm describes adsorption on a single type of uniform pores. A popular equation used in the analysis of isotherms with a high degree of rectangularity is that proposed by Dubinin and Radushkevich

$$q_e = q_s e^{-\beta\varepsilon^2} \tag{12}$$

where q_s is D–R constant and ε can be correlated, the linear form of D–R equation is represented as

$$\log q_e = \log q_s - \beta\varepsilon^2 \tag{13}$$

$$\varepsilon = RT \ln\left[1 + \frac{1}{C_e}\right] \tag{14}$$

where q_e is the amount of Cr(VI) adsorbed per unit weight of the AM-Fe-PGCP (mol/g), q_s is the adsorption capacity (mol/g), β is a constant related to adsorption energy (mol^2/kJ^2), and ε is the Polanyi potential. The adsorption space in the vicinity of a solid surface is characterized by a series of equipotential surfaces having the same adsorption potential. The constant β gives the mean free energy (E) of sorption per molecule of sorbate, when it is transferred to the surface of the solid from infinity in the solution and can be computed using the following relationship

$$E = -\frac{1}{(2\beta)^{1/2}} \tag{15}$$

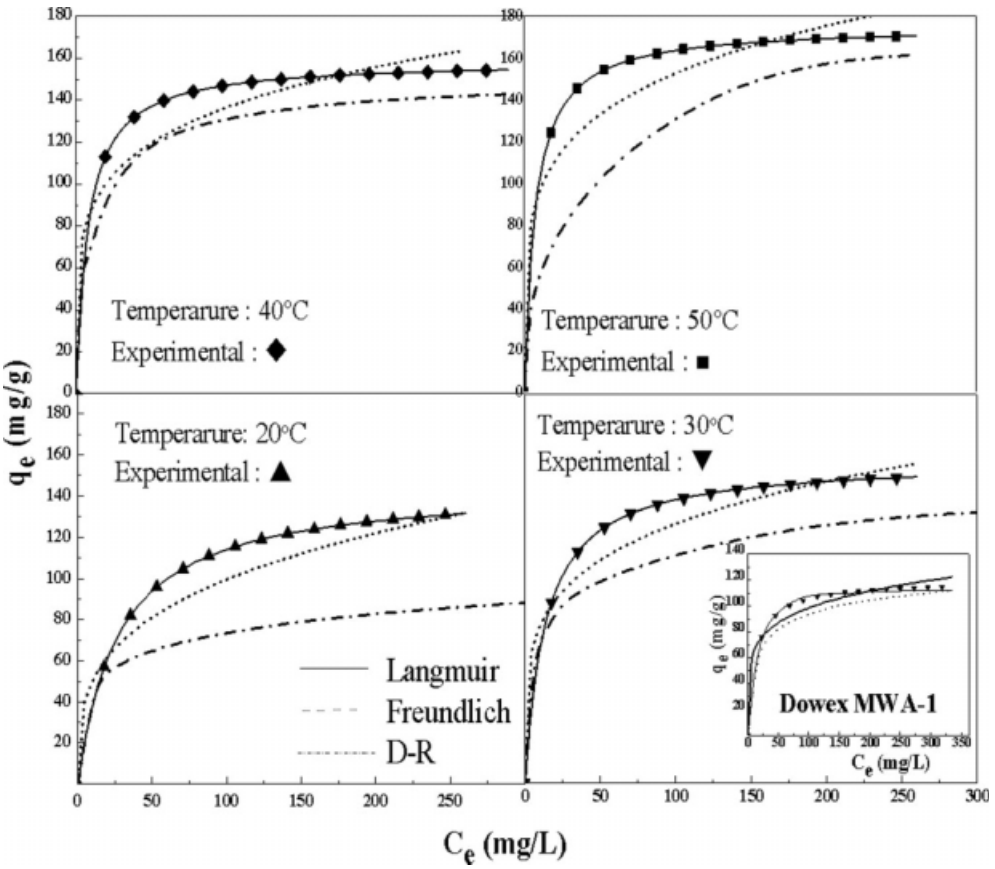

Figure 9 Comparison of experimental and simulated model fits of the various isotherms for the adsorption of Cr(VI) onto AM-Fe-PGCP at different temp and Dowex MWA1 (adsorbent dose 2.0 g/L, equilibrium time 2 h, and pH 4.0).

The value of E is used to estimate the reaction mechanism occurring. The calculated value for Cr(VI) adsorption is 15.8 kJ/mol, which is within the energy range of ion exchange reactions, 8–16 kJ/mol.[40]

All the model parameters were calculated using nonlinear regression analysis and the results are shown in Table II. The calculated isotherm plots using Langmuir, Freundlich, and D–R model parameters in Table II are also shown in Figure 9. It is obvious that the Cr(VI) sorption capacity of AM-Fe-PGCP increased with on rise in temperature, and high capacity was observed at 60°C. As can be seen from Figure 9, the fit is better with Langmuir model than with Freundlich and D–R isotherm models. Based on the highest correlation coefficient (r^2) values of Langmuir isotherm was suggesting that the adsorption process probably dominated by a monolayer adsorption process. Favorability of adsorption was further checked by using a dimensionless separation factor (R_L). The R_L values are in the order $0 < R_L < 1$, $R_L > 1$, $R_L = 1$, and $R_L = 0$ indicates favorable, unfavorable, linear and irreversible, respectively, for the conditions with the shape of isotherms. The values of R_L for adsorption of Cr(VI) at different concentrations (100–600 mg/L) and at different temperatures (30–60°C) were calculated and were found in the range 0.02–0.17. This indicates

TABLE II
Langmuir, Freundlich, and D–R Constants for the Sorption of Cr(VI) Onto AM-Fe-PGCP

	Langmuir				Freundlich				D–R				
Temperature (°C)	Q_0 (mg/g)	b (L/mg)	r^2	χ^2	K_F (mg/g)	n	r^2	χ^2	q_m (mg/g)	$\beta \times 10^{-3}$ (mol^2/kJ^2)	E (kJ/mol)	r^2	χ^2
20	134.5	0.04	0.99	0.22	25.6	3.4	0.95	10.4	90.01	−2.80	13.28	0.95	4.22
30	142.8	0.07	0.98	0.34	43.9	4.6	0.95	11.2	124.75	−2.51	14.12	0.98	3.23
40	158.7	0.12	0.98	0.16	56.4	5.2	0.94	9.23	141.87	−2.21	15.02	0.95	4.61
50	175.4	0.14	0.99	0.51	60.5	5.4	0.93	11.2	161.19	−1.90	15.91	0.97	5.25

that the adsorption process is a very favorable and the adsorbent employed is exhibited a high-adsorption potential.

Thermodynamic study

The temperature dependency onto rate is important to predict the feasibility of the reaction. The nonlinear regression represents a good fit over the entire range of temperatures (30, 40, 50, and 60°C) for pseudo-second-order analysis (Table I). The energy of activation (E_a) for the adsorption process was calculated using the following Arrhenius equation:

$$\ln k_2 = \ln A - \frac{E_a}{RT} \tag{16}$$

where k_2 is rate constant and A is the Arrhenius factor. To extract A and E_a were determined from the slope of ln$k$ versus $1/T$ plot. The values of A and E_a were found to be 88.63 L/mol/s and 22.37 kJ/mol, respectively. The values of the entropy of activation ΔS^* and enthalpy of activation ΔH^* were also determined from the intercept and the slope of the linear plot according to Eyring equation:

$$\ln\left(\frac{k}{T}\right) = \ln\left(\frac{k_b}{h}\right) + \frac{\Delta S^*}{R_g} - \frac{\Delta H^*}{R_g T} \tag{17}$$

where k_b and h are Boltzmann's and Planck's constants, respectively. According to eq. (22), a plot of ln(k/T) versus $1/T$ should be a straight line with a slope $\Delta H^*/R_g$ and intercept [ln(k_b/h) + $\Delta S^*/R_g$]. Gibbs energy of activation (ΔG^*) may be written in terms of entropy and enthalpy of activation:

$$\Delta G^* = \Delta H^* - T\Delta S^* \tag{18}$$

The value of ΔG^* was calculated at 303 K from eq. (23). The values of ΔG^*, ΔH^*, and ΔS^* of activation were found to be 85.03 kJ/mol, 18.37 kJ/mol, and −220.00 J/mol/K, respectively. The positive values of E_a, and ΔG^* suggest the existences of the energy barrier in the exchange reactions. $\Delta G^* > 0$, which means the adsorption of Cr(VI) ions on AM-Fe-PGCP is not spontaneous and need additional energy to complete the adsorption process. Positive value of ΔH^* suggests that the adsorption process is endothermic in nature and this is supported by the increases of Cr(VI)) adsorption onto AM-Fe-PGCP with a rise in temperature, as shown in Figure 9. The negative ΔS^* value indicates that as a result of ion exchange, no significant change occurs in the internal structure of the exchanger.[42] The negative value of ΔS^* also indicates that the Cr(VI) ions at AM-Fe-PGCP are always more organized than those in the bulk solution. It was found that $\Delta H^* > -T\Delta S^*$. This indicates that the influence of enthalpy is more remarkable than entropy of activation. The heat of adsorption determined at constant amounts of sorbate adsorbed is known as the isosteric heat of adsorption (ΔH_x) and is calculated using Clausius–Clapeyron equation.[43]

$$\frac{d(\ln C_e)}{dt} = \frac{-\Delta H_x}{RT^2} \tag{19}$$

The plots of ln C_e versus $1/T$ (figure not shown) for different amounts of Cr(VI) adsorption were found to be linear and the values of ΔH_x were measured from the slopes of the plots. The values of ΔH_x were found to remain almost constant (≈ 51.59 kJ/mol) with increase in surface loading from 30.00 to 70.00 mg/g. This indicates that the surface of AM-Fe-PGCP is energetically more or less homogeneous and the lateral interactions between adsorbed Cr(VI) ions do not exist.

Test with simulated industrial wastewaters

The simulated wastewater was prepared and treated with AM-Fe-PGCP to demonstrate the adsorption potential and utility in removing Cr(VI) from wastewater in presence of other ions. The composition of the wastewater[44] is: Cr(VI), 27.7 mg/L; Cd(II), 3.8 mg/L; CN^-, 12.5 mg/L; Ni(II), 5.1 mg/L; Cu(II), 28.7 mg/L; Zn(II), 4.2 mg/L; chemical oxygen demand, 160.4 mg/L; biological oxygen demand, 49.7 mg/L; suspended solids, 412.5 mg/L; and pH is 4.3. The effect of adsorbent dose on Cr(VI) removal was studied. It is evident that for the quantitative removal of Cr(VI) from 1.0 dm^3 wastewater contain 27.7 mg/L and several other ions; an adsorbent dosage of 0.5 g/L is sufficient for the removal of 99.8% of the total Cr(VI). The efficiency of the adsorbent for the adsorption of Cr(VI) from wastewater is not significantly different from the results predicted on the batch experiments using Cr(VI) only. Under these conditions, the lowest Cr(VI) concentration attained by this material was 0.05 mg/L. The permissible limit of the Cr(VI) for the discharge of industrial wastewater is 0.20 mg/L.

Comparison with other adsorbents

The experimental isotherm data obtained for AM-Fe-PGCP at pH 4.0 and at 30°C were compared with a commercial anion exchanger, Dowex MWA 1 (Fig. 9). The values of Q_0 and b were determined by a nonlinear regression analysis and were found to be 113.87 mg/g and 0.07 L/mg, respectively. In this study, the adsorption capacity of AM-Fe-PGCP has also been compared with that of other adsorbents based on their maximum monolayer sorption capacity for Cr(VI). The Q_0 values

TABLE III
Four Cycles of Cr(VI) Adsorption–Desorption with 0.1*M* NaOH as the Desorbing Agent

	Adsorption		Desorption	
No. of cycles	%	mg/g	%	mg/g
1	96.55	48.27	97.12	46.88
2	94.82	47.41	97.92	46.33
3	93.95	46.98	97.95	46.01
4	92.19	46.10	93.65	43.17

for the adsorption of Cr(VI) onto cationized lignocellulosic material, ammonium functionalized succinylated mercerized celluose, biofilm, chitosan, and ethylenediamine-modified rice hull[45–49] were reported to be 125.5, 43.0, 19.5, and 23.4 mg/g, respectively. The differences of Cr(VI) uptake on various adsorbents are due to the properties(functional groups, surface area, particle size, porosity, etc.) of the adsorbents. The amount of adsorbed Cr(VI) at 30°C was high enough for AM-Fe-PGCP (142.76 mg/g) to be able to effectively remove Cr(VI) from wastewater.

Desorption and regeneration studies

The use of an adsorbent in the wastewater treatment depends not only on the adsorption capacity, but also on how well the exhausted adsorbent can be regenerated and used again. To test repeatedly using the adsorbent and to recover the chromium(VI), the recovery and regeneration tests were conducted with different types of desorbing agents (NaOH, Na_2SO_4, NaCl, $NaNO_3$, HCl, and HNO_3) through batch technique. Desorption of Cr(VI) from AM-Fe-PGCP was 67.4, 72.5, 78.8, 85.6, and 96.6% with 0.001, 0.005, 0.01, 0.05, and 0.1*M* NaOH, respectively. From these results, it may be concluded that ligand exchange is occurring in the adsorption process. The adsorption–desorption cycles were repeated for four cycles using 0.1 g of the adsorbent and 50 mL of 100 mg/L Cr(VI) solution for adsorption and desorption was carried out with 50 mL of 0.1*M* NaOH. The results of regeneration study of Cr(VI) by NaOH solution are shown in Table III. After four cycles, the adsorption capacity of AM-Fe-PGCP decreased from 48.27 mg/g (96.6%) to 46.10 mg/g (92.2%), while the recovery of Cr(VI) decreased from 97.1% in the first cycle to 93.7% in the fourth cycle. After each desorption experiments, we re-introduced Fe^{3+} to restore the adsorption sites, almost same as the original values and subsequent adsorption experiments were conducted using re-introduced Fe^{3+} in AM-Fe-PGCP (AM-re-Fe-PGCP). The amount of Fe^{3+} restored in the regenerated adsorbent after removal of Cr(VI) by NaOH treatment was 8.7, 9.5, 9.8, and 8.4 mg/g in the first, second, third, and fourth cycle, respectively. The regenerated adsorbent showed uptake efficiency comparable with that of the fresh ones over four cycles. The results show that even after four cycles of sorption and desorption, there was no appreciable decrease in the sorption capacity of AM-Fe-PGCP. This indicated that the material could be reused for four to five times for the sorption of Cr(VI).

CONCLUSIONS

The ability of a newly developed adsorbent, iron(III) coordinated amino-functionalized polyacrylamide-grafted coconut coir pith (AM-Fe-PGCP) to adsorb Cr(VI) from aqueous solutions was investigated under various experimental conditions. FTIR, EDS, Mössbauer, surface area analyzer, TG/DTG, and potentiometric titration were used to characterize the adsorbent. Sorption of Cr(VI) is pH-dependent and the best results were obtained at pH 4.0. Equilibrium adsorption time was found to be 2 h and the kinetics of the sorption process was found to follow the pseudo-second-order rate law. Film diffusion mechanism plays a significant role in the adsorption process. Thermodynamic constants were also evaluated using Eyring equation. The isotherm data were correlated well by Langmuir model when compared with Freundlich and D–R isotherm models. Using the Langmuir model, the maximum monolayer adsorption capacity of AM-Fe-PGCP was found to be 142.76 mg/g at 30°C. Energy parameters from the D–R isotherm indicate the ligand exchange mechanism for adsorption. Quantitative removal of 27.7 mg/L Cr(VI) in 1.0 L of electroplating industry wastewater was achieved by 0.5 g of the adsorbent at pH 4.0 and 30°C. The alkali treatment (0.1*M* NaOH) and re-incorporation of Fe^{3+} lead to a reactivation of the used adsorbent and the adsorbent can be reused for several cycles, consecutively without noticeable loss of capacity. The results of this study suggest that AM-Fe-PGCP exhibits significant potential as an adsorbent in the removal of Cr(VI) from aqueous solutions and industrial wastewaters.

References

1. Chiarle, S.; Ratto, M.; Rovatti, M. Water Res 2000, 34, 2971.
2. Environmental Protection Agency (EPA). Available at: http://www.epa.gov. (accessed 1996).
3. Babel, S.; Kurniawan, T. A. J Hazard Mater 2003, B97, 219.
4. Mohan, D.; Pittman, C. U. J Hazard Mater 2007, 142, 1.
5. Amin, M. N.; Kaneco, T.; Begum, A.; Katsumata, H.; Suzuki, T.; Ohta, K. Ind Eng Chem Res 2006, 45, 8105.
6. Shibi, I. G.; Anirudhan, T. S. J Chem Technol Biotechnol 2006, 81, 433.
7. Noelin, B. F.; Manohar, D. M.; Anirudhan, T. S. Sep Purif Technol 2005, 45, 131.
8. Abdel-Aal, S. E.; Gad, Y. H.; Dessouki, A. M. J Appl Polym Sci 2006, 99, 2460.

9. Bicak, N.; Sherrington, D. C.; Senkel, B. F. React Funct Polym 1999, 41, 69.
10. Shibi, I. G.; Anirudhan, T. S. Chemosphere 2005, 58, 1117.
11. Anirudhan, T. S.; Unnithan, M. R.; Divya, L.; Senan., P. J Appl Polym Sci 2007, 104, 3670.
12. Caulfield, M. J.; Qiao, G. G.; Solomon, D. H. Chem Rev 2002, 102, 3067.
13. Flory, P. J. Principles of Polymer Chemistry; Cornell University Press: Ithaca, NY, 1953.
14. Hsien, J. Y.; Rorrer, G. C. Ind Eng Chem Res 1997, 36, 3631.
15. Zhou, Y.; Ya, C.; Shan, Y. Sep Purif Technol 2004, 36, 89.
16. Pearson, R. G. Science 1966, 151, 172.
17. Mathew, B.; Pillai, V. N. R. Polymers 1993, 34, 2650.
18. Fryxell, G. E.; Liu, J.; Hauzao, T. A.; Nia, E.; Ferris, K. F.; Mattigod, S.; Gong, M.; Hallen, R. T. Chem Mater 1999, 11, 2148.
19. Swaddle, T. W. Inorganic Chemistry; Academic Press: New York, 1997.
20. Anirudhan, T. S.; Unnithan, M. R. Chemosphere 2007, 66, 60.
21. Ott, E. Cellulose and Cellulose Derivatives; Interscience Publishers: NewYork, 1946.
22. Schwarz, J. A.; Driscoll, C. T.; Bhanot, A. K. J Colloid Interface Sci 1984, 97, 55.
23. Zhu, X.; Alexandratos, S. D. Ind Eng Chem Res 2005, 44, 8605.
24. Greenberg, A. E.; Clescerl, L. S.; Eaton, A. D. Standard Method for the Examination of Water and Wastewater; 18th ed.; APHA, AWWA, and WEF: Washington, DC, 1992.
25. Giles, C. H.; Mcewane, T. H.; Nakhwa, S. N.; Smith, D. J Chem Soc 1960, 4, 3973.
26. Hawthorne, F. C. In Spectroscopic Methods in Mineralogy and Geology, Reviews in Mineralogy; Hawthorne, F. C., Ed.; Mineral Society of America: Washington, 1988; Vol. 18, p 255.
27. Mccammon, C. A. In Spectroscopic Methods in Mineralogy. EMU Notes Mineral; Beran, A.; Libowitzky, E., Eds.; Eötvös University Press: Budapest, 2004; Vol. 6, p 369.
28. Dyar, M. D. Am Miner 1984, 69, 1127.
29. Burns, R. G. Hyperfine Int 1994, 91, 739.
30. Ornek, A.; Ozacar, M.; Sengal, I. A. Biochem Eng J 2007, 37, 192.
31. Ramos, R. L.; Martinez, J.; Coronado, R. M. G. Water Sci Technol 1994, 30, 191.
32. Kotaś, J.; Stasicka, Z. Eniron Poll 2000, 107, 263.
33. Benefield, L. D.; Judkins, J. P.; Wend, B. L. Chem Zentr 1982, 1, 875.
34. Hamadi, N. K.; Chen, X. D.; Farid, M. M.; Lu, M. G. Q. Chem Eng J 2001, 84, 95.
35. Quintana, A.; Curutehat, G.; Donate, E. Biochem Eng J 2001, 9, 11.
36. Anirudhan, T. S.; Suchithra, P. S. Ind Eng Chem Res 2007, 46, 4606.
37. Ho, Y. S.; Mckay, G. Water Res 2000, 34, 135.
38. Marquardt, D. W. J Soc Ind Appl Math 1963, 11, 431.
39. Bhattacharya, A. K.; Venkobacher, C. J Env Eng Div ASCE Proc 1984, 110, 110.
40. Helfferich, F. Ion Exchange; McGraw–Hill: New York, 1962.
41. Cimino, G.; Passerini., A. Water Res 2000, 34, 2955.
42. Brito, F.; Ascanio, J.; Mateo, S.; Hernandez, C.; Araujo, L.; Gili, P.; Martin-Zarza, P.; Dominguez, S.; Mederos., A. Polyhedron 1997, 16, 3835.
43. Young, D. M.; Crowell, A. D. Physical Adsorption of Gases; Butterworth: London, 1962.
44. Maya, R.; Vinod, V. P.; Anirudhan, T. S. Ind Eng Chem Res 2004, 43, 2247.
45. Zghida, H.; Baouab, M. H. V.; Gauthier, R. J Appl Polym Sci 2003, 87, 1660.
46. Gurgel, L. V. A.; De Melo, J. C. P.; De Lena, J. C.; Gil, L. F. Bioresour Technol 2009, 13, 3214.
47. Quintelas, C.; Fernandes, B.; Castro, J.; Figueiredo, H.; Tavares, T. Chem Eng J 2008, 136, 195.
48. Schmuhl, R.; Krieg, H. M.; Keizer, K.; Water, S. A. 2001, 27, 1.
49. Tang, P. L.; Lee, C. K.; Low, K. S.; Zainal, Z. Environ Technol 2003, 24, 1243.